PHYSICAL REVIEW B VOLUME 59, NUMBER 13 1 APRIL 1999-I

Anomalous transition from antiferromagnetic to ferromagnetic order in $Tb_{1-x}Y_xNiAl$

G. Ehlers*
Hahn-Meitner-Institut Berlin, Glienicker Strasse 100, 14109 Berlin, Germany

C. Ritter
Institut Laue-Langevin, Boîte Postale 156, 38042 Grenoble, France

A. Krutjakow, W. Miekeley, N. Stüßer, Th. Zeiske, and H. Maletta
Hahn-Meitner-Institut Berlin, Glienicker Strasse 100, 14109 Berlin, Germany

(Received 19 May 1998; revised manuscript received 9 November 1998)

We shall describe the change of magnetic order occurring in the pseudo-ternary system $Tb_{1-x}Y_xNiAl$, which was investigated in the range of $0 \leqslant x \leqslant 0.8$ by ac- and dc-susceptibility measurements and neutron diffraction experiments. An anomalous transition from antiferromagnetic to ferromagnetic order was observed. Characteristic features of the transition are (a) it occurs in a narrow range of the Y content between $x = 0.01$ and $x = 0.05$, (b) both types of magnetic order *coexist* in different domains of the same compound, and (c) the preferred type of order changes with temperature. [S0163-1829(99)01113-3]

I. INTRODUCTION

Intermetallic compounds of elements with partially filled *f*-electron shells have received a lot of attention in recent years, because of their unusual magnetic properties at cryogenic temperatures. Numerous effects such as the Kondo effect, heavy fermion behavior, coexistence of superconductivity and long range magnetic order, mixed valence and complex magnetic ordering have been studied and the results were of importance to theory as well as to applications. The class of ternary intermetallic compounds includes large isostructural families such as the group of orthorhombic TiNiSi (space group $Pnma$)[1] or that of hexagonal Fe_2P (space group $P\overline{6}2m$).[2] In ternary compounds the latter structure often appears as the ZrNiAl structure,[3,4] which is an ordered derivative of the Fe_2P structure. Extensive and systematic investigations of $4f$- and $5f$-electron systems were carried out in changing stoichiometry and thus modifying the chemical and electronic environments,[5,6] while the crystal structure remained unchanged.

In ternary compounds of the Fe_2P structure the rare earth (if present) always occupies the site $3g$. The symmetry of the triangular lattice of this site in the ab plane resembles that of the *kagomé* lattice[7] (see Fig. 1). Theoretical studies have revealed the absence of long range magnetic order in antiferromagnetic arrangements of localized Ising spins on a two-dimensional *kagomé* lattice and on other triangular lattices, which is due to inherent frustration.[7,8] Compounds of the Fe_2P structure are three-dimensional systems (though in general with a strong magnetic anisotropy) and thus antiferromagnetic order may occur in the ab plane, although a topological frustration can of course be expected.

This phenomenon occurs in the antiferromagnetic compounds of the RNiAl series, which crystallize in the hexagonal Fe_2P structure. Bulk measurements (magnetization, electrical resistivity, specific heat) showed that RNiAl compounds are characterized by a complex magnetic behavior[9–11] and this finding was confirmed later by neutron diffraction studies.[12–17]

TbNiAl was the first compound of this series, in which the authors[12,13] observed frustration effects on the magnetic ordering of the Tb moments by detailed neutron scattering experiments. The magnetic structures of TbNiAl will briefly be described in Sec. III C. All Tb moments are found to

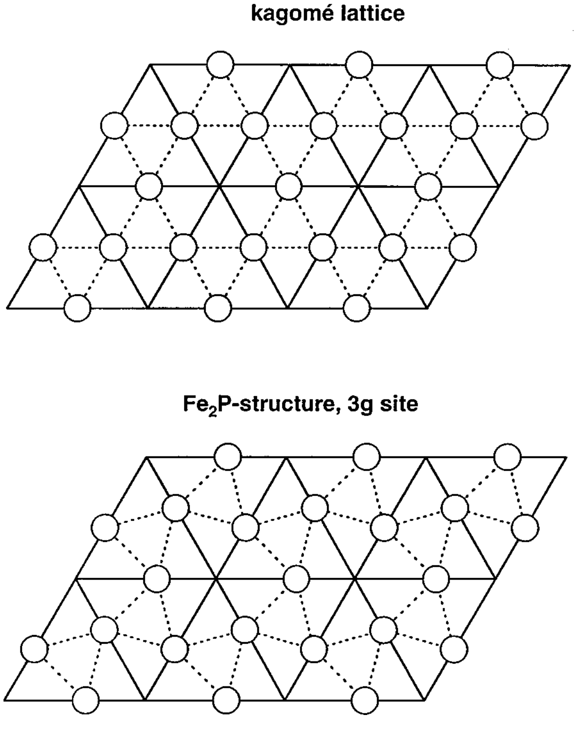

FIG. 1. The *kagomé* lattice (upper panel) and the lattice formed by the rare earth site ($3g$) in the Fe_2P structure (lower panel). The site parameter $x_{Tb} = 0.59$, which is found in TbNiAl, was used to draw the lower panel. A value of $x_{Tb} = 0.5$ would actually correspond to the real *kagomé* lattice. The dashed lines are guides to the eye.

0163-1829/99/59(13)/8821(7)/$15.00

order antiferromagnetically, but the topological frustration effect considerably reduces the size of 1/3 of the ordered moments. In the hexagonal system CePdAl (Ref. 18) even stronger frustration effects were observed: 1/3 of the magnetic Ce moments remain paramagnetic in the antiferromagnetically ordered state. In isostructural $5f$-compounds antiferromagnetic coupling only occurs between adjacent ab planes, and thus no frustration is observed. Only recently a notable exception has been reported: In UNiAl [magnetic propagation vector $\boldsymbol{k}_m=(0.1,0.1,0.5)$] the spin structure shows a similar frustration effect in the basal plane.[19]

In a previous paper we showed that in TbNiAl the antiferromagnetic coupling between nearest neighbors of Tb moments can be changed to ferromagnetic coupling by substituting a small amount of Ni by Cu.[20] The magnetic coupling processes in a complicated system, in which different interactions compete, can be studied by replacing the magnetic atom (Tb) with a nonmagnetic one (Y). Y is known to be a suitable substitute for Tb in crystals, and in fact YNiAl is isostructural to TbNiAl and its lattice parameters are similar.[3] It was therefore expected that the substitution would not affect the crystal structure, and we would thus be able to systematically study the effect of magnetic dilution.

II. EXPERIMENT

For sample preparation Tb of a purity of 99.9% purchased from Johnson Matthey was used. The other metals were of a purity of at least 99.99%. Samples containing Y in the amount ranging from $x=0$ to $x=0.80$ were synthesized by inductive levitation melting of the pure elements in argon atmosphere. To guarantee for homogeneity, the buttons were turned over and remelted several times and then annealed in quartz tubes in a vacuum at a temperature of 800 °C for 120 h. Finally the buttons were crushed to a fine powder and examined at room temperature by Cu-K_α radiation x-ray diffraction. In order to control the 2θ scale and the resolution function of the diffractometer, NBS Si standard powder was added to the samples for these measurements. This procedure guaranteed a good statistical mixture of Tb and Y in the samples (see below). The ac susceptibility was measured with a Lake Shore ac susceptometer (model 7221), equipped with a 1 T magnet, which covers a temperature range from liquid helium to room temperature. For dc-magnetization measurements a Quantum Design SQUID magnetometer MPMS with a 5.5 T magnet was used. To avoid reorientation of the grains during the measurement, small powder samples prepared with nonmagnetic glue were used. Neutron diffraction experiments were performed at the D1B powder diffractometer at ILL, Grenoble,[21] at an incident neutron wavelength of $\lambda=2.52$ Å, as well as at the diffractometers E2 and E6 at HMI, Berlin[22] ($\lambda=2.40$ Å). During these experiments the wavelength was determined precisely for each single measurement by a standard YIG sample.

In some compounds which contain Y a spurious contamination with an unknown foreign phase was visible in neutron diffraction patterns. The intensity of the weak Bragg peaks due to this phase did not change with temperature suggesting that it was not magnetic. From peak intensities the volume fraction of the foreign phase could roughly be estimated, and since it did not exceed 1%, it does not affect our study.

The diffraction data were analyzed by the Rietveld method[23] with the help of the computer program FULLPROF,[24] which handles x-ray and neutron data. In Rietveld refinement, the measured diffraction pattern is directly fitted to a model pattern calculated by the program using parameters describing (1) the instrument (wavelength, linewidth, line shape) and (2) the sample (space group, atom parameters, lattice constants, magnetic moments). For the analysis of the x-ray data, atomic scattering factors of the different ions were used, which are stored in internal tables of the program. The neutron data were analyzed using scattering lengths from standard tables.[25] The magnetic form factor of Tb^{3+} was taken from another standard reference.[26] The dipolar approximation $f_k=\langle j_0\rangle+c_2\langle j_2\rangle$ was used ($c_2=1/3$ for Tb^{3+}). In order to determine the ordered magnetic moments precisely, the magnetic and crystal structures were analyzed simultaneously in the neutron diffraction patterns. To obtain consistent results for the crystal structures from both the x-ray and neutron data, additional neutron patterns were measured in the paramagnetic phases.

III. RESULTS

A. X-ray scattering results

The x-ray diffraction experiments were performed at room temperature in order to check the quality of the samples. The lattice constants of all compounds corresponded to previously published results and the parameters of the atom sites were in accordance with the $\mathrm{Fe_2P}$ structure. For example, in $\mathrm{Tb_{0.50}Y_{0.50}NiAl}$ at $T=295$ K we found $a=7.0186(4)$ Å and $c=3.8538(3)$ Å. The atom positions are

$$\text{Tb/Y:}\quad \text{at } 3g\ \ (x0\tfrac{1}{2}),\ (0x\tfrac{1}{2}),\ (\overline{x\,x}\tfrac{1}{2})$$

$$\text{Al:}\quad \text{at } 3f\ \ (x00),\ (0x0),\ (\overline{x\,x}0)$$

$$\text{Ni}_\text{I}:\quad \text{at } 2c\ \ (\tfrac{1}{3}\tfrac{2}{3}0),\ (\tfrac{2}{3}\tfrac{1}{3}0)$$

$$\text{Ni}_\text{II}:\quad \text{at } 1b\ \ (00\tfrac{1}{2}).$$

The site parameters are $x_\mathrm{Tb}=0.586(3)$ and $x_\mathrm{Al}=0.21(4)$. In the prototype compound $\mathrm{Fe_2P}$ Fe occupies the $3g$ as well as the $3f$ position, whereas Tb/Y and Al are well separated in both sites. The atoms form a layered structure, in which Tb/Y-Ni and Al-Ni planes alternate along the hexagonal c axis.

We should like to emphasize that the samples are homogeneous. The rare earth occupies its own site in the crystal structure, but it is possible that clusters are formed during sample preparation. These clusters could be enriched in Tb or Y with respect to the nominal concentration of both metals. This would be indicated by broadened Bragg peaks in x-ray diffraction, because the lattice constants of pure TbNiAl and YNiAl differ in the order of 1%. Bragg reflections at slightly different q values due to clusters with different lattice constants could easily be resolved by a Guinier diffractometer. In the x-ray data there is no qualitative difference between the line shape of pure TbNiAl and the pseudoternary compounds. The measured linewidth typically is somewhat larger than that of the NBS Si standard (see upper panel of Fig. 2). In addition, Fig. 2 shows that the

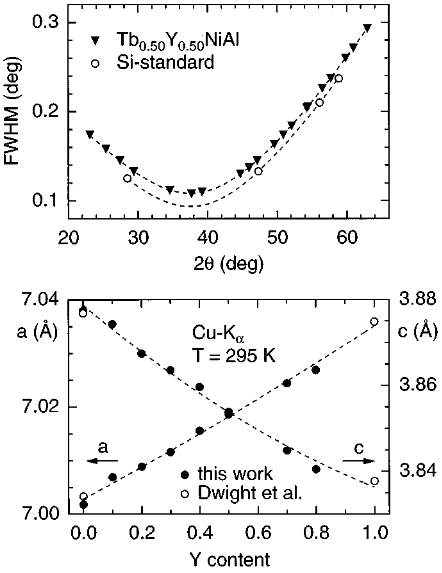

FIG. 2. Overview of the x-ray data obtained for the series $Tb_{1-x}Y_xNiAl$. The measured linewidth (FWHM) is shown for a representative compound and the NBS Si standard (upper panel). The composition-dependent lattice constants (measured at room temperature) are given in the lower panel. Note that a increases with increasing Y content x whereas c decreases. The data from Dwight *et al.*[3] for TbNiAl and YNiAl are included. The dashed lines are guides to the eye.

lattice parameters, as determined by x-ray diffraction at room temperature, vary quite smoothly with changing Y content x. The values we obtained are in agreement with those given by Dwight *et al.*,[3] which are also included in Fig. 2. Therefore it is to be assumed that the samples contain a good statistical mixture of Tb and Y.

B. Magnetic bulk measurements

Magnetization measurements show that with increasing Y content the magnetic ordering temperature slowly decreases from the Néel temperature $T_N = 47$ K in TbNiAl to the Curie temperature $T_C = 14$ K in $Tb_{0.20}Y_{0.80}NiAl$ over the entire $Tb_{1-x}Y_xNiAl$ series. Compounds with $x \leqslant 0.03$ are antiferromagnetic while all others are ferromagnetic. The type of magnetic order changes at a Y content between $x = 0.01$ and $x = 0.05$. To illustrate the change from antiferromagnetic to ferromagnetic order, we shall now compare the compounds $Tb_{0.99}Y_{0.01}NiAl$ and $Tb_{0.95}Y_{0.05}NiAl$. The susceptibility of both compounds, measured in a constant magnetic field of $B = 100$ G at increasing temperature, is given in the upper panel of Fig. 3. Both compounds have the same ordering temperature $T_C = 47$ K. The field-cooled (FC) and the zero-field-cooled (ZFC) susceptibility were measured. It was found that the ZFC susceptibility is generally lower and due to the motion of domain walls[27] time dependent. When the compound is cooled through its ordering point in zero field, an irregular domain structure is established and the direction of the spontaneous magnetization is locally determined by magnetic anisotropy. When the field is switched on and the sample is warmed up, the domain walls start moving and the magnetization of different domains turns into the energetically most favorable direction, which is also influenced by the external magnetic field.

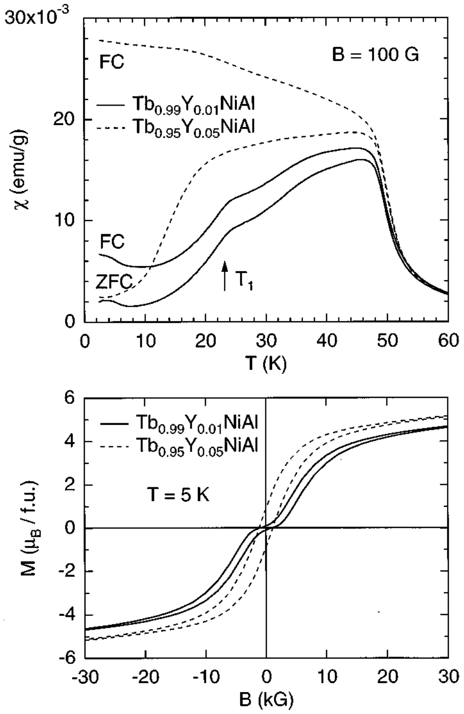

FIG. 3. The dc susceptibility of $Tb_{0.99}Y_{0.01}NiAl$ and $Tb_{0.95}Y_{0.05}NiAl$ measured at increasing temperature in a constant magnetic field of $B = 100$ G (with both FC and ZFC history) is shown in the upper panel. At the temperature T_1 a change in the antiferromagnetic order of $Tb_{0.99}Y_{0.01}NiAl$ occurs. In the lower panel the magnetization curves of the same compounds at a constant temperature of $T = 5$ K are given.

The maximum FC susceptibility of $Tb_{0.99}Y_{0.01}NiAl$ is measured close to the ordering temperature which characterizes antiferromagnets, whereas in $Tb_{0.95}Y_{0.05}NiAl$ the maximum susceptibility is reached at low temperature (Fig. 3). In $Tb_{0.99}Y_{0.01}NiAl$ another magnetic transition occurs at $T_1 = 23$ K. This second transition also occurs in pure antiferromagnetic TbNiAl (see Sec. III C). The magnetization of both compounds measured at a constant temperature of $T = 5$ K (see right panel of Fig. 3) results in consistently lower values of the remanence and coercive field for antiferromagnetic $Tb_{0.99}Y_{0.01}NiAl$.

In Tb rich samples with $x \leqslant 0.15$ a double peak structure develops in the ac susceptibility when a constant magnetic field is applied (not shown as a figure). The high temperature peak is shifted to higher temperatures when the external field is increased. At the same time the low temperature peak moves to lower temperatures and vanishes at about $B = 5$ kG. We interpret these observations as an indication of competing ferro- and antiferromagnetic correlations, respectively, existing up to about $x = 0.15$.

C. Neutron scattering results

In this section we shall first consider two compounds, which are outside of the range where the change of magnetic order occurs: pure TbNiAl, which is antiferromagnetic, and $Tb_{0.50}Y_{0.50}NiAl$, which is ferromagnetic. Then we shall

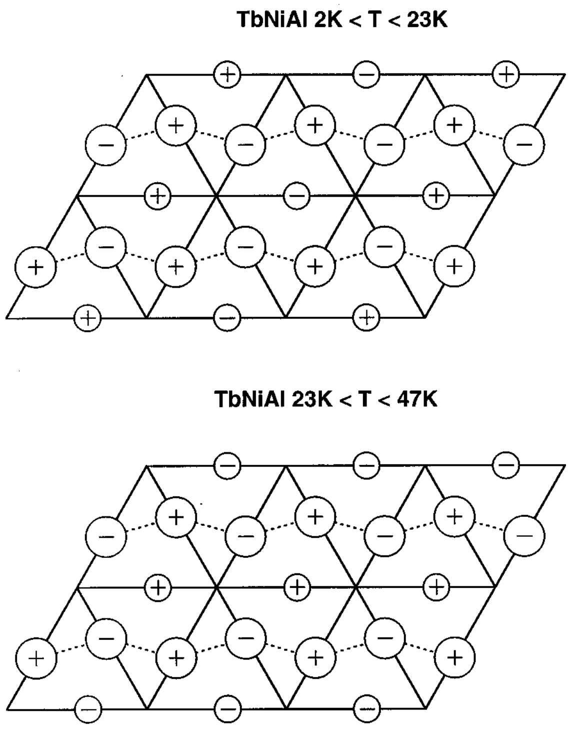

FIG. 4. The two ordered magnetic structures which occur in TbNiAl. Upper panel: the temperature range 2 K$\leqslant T \leqslant$23 K; lower panel: 23 K$\leqslant T \leqslant$47 K. Large circles correspond to regular moments. These moments form zigzag chains (dashed lines) which are separated by frustrated moments (small circles). Above $T=23$ K frustrated moments are reduced in size.

present our results in the transition range, showing how the transition takes place at a fixed temperature, when the stoichiometry is changed, as well as at a fixed stoichiometry with changing temperature.

The results on the magnetic structure of pure TbNiAl (Refs. 12–14) will briefly be summarized here. A commensurate antiferromagnetic propagation vector $\boldsymbol{k}_1^{(\mathrm{afm})}=(\frac{1}{2}\frac{1}{2}\frac{1}{2})$ was found in TbNiAl below $T_N=47$ K. In the hexagonal system for the site 3g the propagation vector belongs to a star of three arms: $\boldsymbol{k}_1^{(\mathrm{afm})}=(\frac{1}{2}\frac{1}{2}\frac{1}{2})$, $\boldsymbol{k}_2^{(\mathrm{afm})}=(\bar{\frac{1}{2}}0\frac{1}{2})$ and $\boldsymbol{k}_3^{(\mathrm{afm})}=(0\bar{\frac{1}{2}}\frac{1}{2})$. Throughout the paper antiferromagnetic reflections will be written using $\boldsymbol{k}_1^{(\mathrm{afm})}$. In a powder diffraction experiment independent nuclear reflections and magnetic satellites from different peaks may overlap at identical scattering angles, and thus make it impossible to separate the contributions from different reflections arriving at a single detector. Certain (hkl) values were therefore taken to represent all reflections at the same point. For example, we write (101) for the reflections (101), $(\bar{1}01)$, (011), $(0\bar{1}1)$, $(1\bar{1}1)$, $(\bar{1}11)$, and we write $(\frac{1}{2}\frac{1}{2}\frac{1}{2})$ for $(\frac{1}{2}\frac{1}{2}\frac{1}{2})$, $(\bar{\frac{1}{2}}\,\bar{\frac{1}{2}}\,\bar{\frac{1}{2}})$, $(\frac{1}{2}0\frac{1}{2})$, $(\bar{\frac{1}{2}}0\frac{1}{2})$, $(\frac{1}{2}0\bar{\frac{1}{2}})$, $(\bar{\frac{1}{2}}0\bar{\frac{1}{2}})$. The symbol $(\frac{3}{2}\frac{1}{2}\frac{1}{2})$ represents 12 single reflections.

In TbNiAl all magnetic moments are aligned either parallel or antiparallel to the c axis. In the temperature range 23 K$\leqslant T \leqslant$47 K the structure shown in the lower panel of Fig. 4 is found. Two antiferromagnetic sublattices are established and can be distinguished by the size of the ordered Tb moments. Note that along the c axis the coupling between nearest neighbors is also antiferromagnetic. Two thirds of the Tb moments are ordered antiferromagnetically along zigzag chains in the hexagonal ab plane (large circles in Fig. 4). We call them regular moments in order to distinguish them from the other third of Tb moments. The zigzag chains separate linear chains formed by the other third of Tb moments which are strongly reduced in size and hence called frustrated (small circles in Fig. 4). For example, at $T=40$ K we found $\mu=(4.9\pm0.1)\mu_B$ for the regular moments and $\mu=(0.8\pm0.1)\mu_B$ for the frustrated moments. A second magnetic transition takes place at $T_1=23$ K, where the sublattice of the frustrated moments changes from ferromagnetic chains to antiferromagnetic chains parallel to the regular moment chains. Below $T_1=23$ K the size of the frustrated moments is less reduced, and at $T=2$ K all moments have the same size: $\mu=(8.0\pm0.1)\mu_B$.

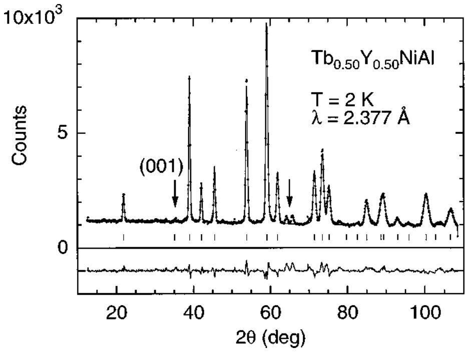

FIG. 5. The neutron powder diffraction pattern of $\mathrm{Tb_{0.50}Y_{0.50}NiAl}$ measured at E6 (HMI Berlin) at a temperature of $T=2$ K. The position of the (001) peak, which has little nuclear and no magnetic intensity, is indicated. The right arrow points to the strongest peaks due to a foreign phase. Below the calculated difference between the measured and the refined profiles is given using the same intensity scale.

Among all possible magnetic structures with the same propagation vector $\boldsymbol{k}_1^{(\mathrm{afm})}$ only the structures presented in Fig. 4 were found to correspond to the experimentally observed magnetic Bragg intensities. These results for TbNiAl are supported by a high statistical significance of the fitted profiles. The Rietveld refinement typically converges at R factors between 3% and 5% for both the crystal and the magnetic structures. Any microscopic model for the magnetic structure, that assumes the same size for all magnetic moments, fails above $T=10$ K ($R_{\mathrm{mag}}>10\%$). A model with a spin direction different from the c-axis direction does not give any good fit either. This is in agreement with previously published magnetization measurements on a single crystal of TbNiAl which show that the c axis is the easy axis.[14]

$\mathrm{Tb_{0.50}Y_{0.50}NiAl}$ is a ferromagnetic Ising system with a Curie temperature of $T_C=32$ K. Figure 5 shows the refined diffraction pattern at $T=2$ K. Magnetic Bragg peaks are only observed on top of the structural Bragg peaks. The fit converged at $\chi^2=5.41$, giving R factors of $R_{\mathrm{nucl}}=4.4\%$ and $R_{\mathrm{mag}}=4.9\%$. The ordered magnetic moment at this temperature is $\mu=(7.6\pm0.2)\mu_B$. Note, that there is no (001) peak at $2\theta=35.9°$ (since the nuclear intensity is negligibly small).

We shall now discuss neutron diffraction measurements of compounds, which show the transition from antiferromag-

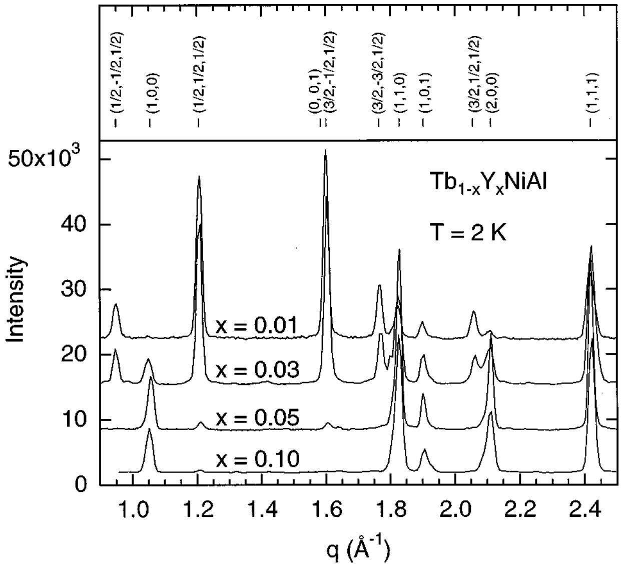

FIG. 6. Low-angle parts of neutron diffraction patterns taken at $T=2$ K for different stoichiometries (raw data). Four curves corresponding to values $x=0.01$, $x=0.03$, $x=0.05$, and $x=0.10$ of the Y content are given. Momentum transfer q rather than scattering angle 2θ was chosen as x axis, because the patterns were measured at different diffractometers. For the same reason, the actual count rates were multiplied by factors to give a common intensity scale. The reflection markers can be taken for all four compounds, because the lattice constants of the samples are similar.

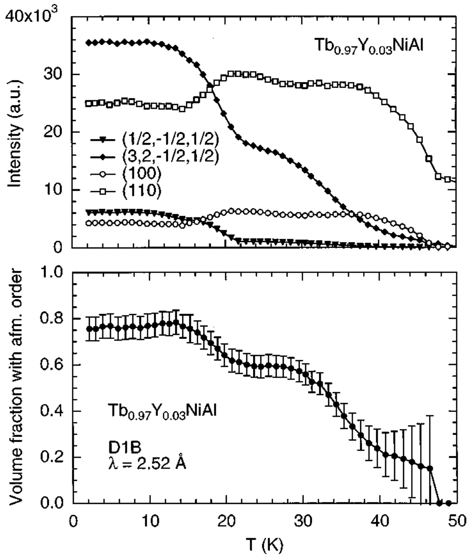

FIG. 7. Temperature dependence of prominent observed magnetic Bragg peaks of $Tb_{0.97}Y_{0.03}NiAl$ (D1B data, upper panel). Half-integer Bragg peaks are represented by full symbols; integer Bragg peaks are open symbols. The related volume ratio V_{afm}/V_{total} is shown in the lower panel.

netic to ferromagnetic order. Figure 6 shows the low-angle parts of the neutron diffraction patterns measured at $T=2$ K for four compounds with $x=0.01$, $x=0.03$, $x=0.05$, and $x=0.10$ (raw data). Bragg indices are also included in the figure. They can be taken for all four compounds, because the lattice constants are similar. However, these are considerably different compared to the measurements at room temperature. For example, for $Tb_{0.95}Y_{0.05}NiAl$ at $T=2$ K we found $a=6.872(1)$ Å and $c=3.968(1)$ Å. At $T=2$ K, the constant a is about 2% smaller and c is about 2% larger than at room temperature. This anisotropic change of the lattice constants will briefly be discussed at the end.

In $Tb_{0.99}Y_{0.01}NiAl$ the same antiferromagnetic structure as in TbNiAl and the same magnetic transition from one type of structure to the other at $T_1=23$ K were observed. No ferromagnetic intensity was observed on top of the structural Bragg peaks. In contrast, in $Tb_{0.95}Y_{0.05}NiAl$ ferromagnetic order is dominant. In this compound we found the same magnetic structure factors as in $Tb_{0.50}Y_{0.50}NiAl$ (see above). There is no magnetic (001) peak. However, the neutron diffraction experiment shows, that $Tb_{0.95}Y_{0.05}NiAl$ actually is not a pure ferromagnet as the magnetization curve suggested. At scattering angles corresponding to the two most intense antiferromagnetic reflections $(\frac{1}{2}\frac{1}{2}\frac{1}{2})$ and $(\frac{3}{2}\frac{1}{2}\frac{1}{2})$ two small peaks can still be observed. This leads to the conclusion that a part of $(5\pm1)\%$ of the total volume of $Tb_{0.95}Y_{0.05}NiAl$ still orders in antiferromagnetic domains. The Rietveld refinement shows that at $T=2$ K in the four compounds of Fig. 6 all ordered magnetic Tb moments are of the same size: $\mu=(7.9\pm0.2)\mu_B$. The possibility that the weak half-integer peaks observed in $Tb_{0.95}Y_{0.05}NiAl$ are due to a λ/2 contamination of the neutron beam can be ruled out. This measurement was performed at D1B, where the second order contamination amounts to about $(2-5)\times10^{-4}$.

We shall now consider the compound $Tb_{0.97}Y_{0.03}NiAl$, in which another aspect of the AFM-FM transition becomes apparent, because neither of the structures is strongly dominant. Here intensities of both groups of Bragg reflections, corresponding to $\boldsymbol{k}_1^{(afm)}=(\frac{1}{2}\frac{1}{2}\frac{1}{2})$ (antiferromagnetic order) and $\boldsymbol{k}^{(fm)}=(000)$ (ferromagnetic order) are comparable. On a microscopic scale different situations may occur and lead to the same experimental observation: (1) magnetic order is ferrimagnetic and uniform in the whole compound or (2) different parts of the sample, i.e., domains, have different magnetic order.

In a neutron diffraction experiment these two scenarios cannot be distinguished unless any supplementary argument is found. Information about substructures corresponding to different propagation vectors $\boldsymbol{k}$ is obtained at different scattering angles. Thus the data can easily be analyzed separately. If a ferrimagnetic structure is assumed and the net moment of both sublattices is written as $A\pm B$, where A corresponds to the ferromagnetic and B to the antiferromagnetic intensity, we arrive at $A=(3.8\pm0.1)\mu_B$ and $B=(6.2\pm0.2)\mu_B$ for $Tb_{0.97}Y_{0.03}NiAl$ at $T=2$ K. Since Tb cannot obtain a moment of $\mu=A+B=10.0\mu_B$ (the maximum value for the Tb^{3+} ion is $g_J J=9.0\mu_B$), a ferrimagnetic order can be ruled out, and it is to be concluded that different domains of both types of order coexist. At higher temperatures, where the ordered moments are smaller, this argument does not lead to a contradiction, but it seems very unlikely that a change from scenario (1) to (2) would occur at some intermediate temperature.

The integrated magnetic Bragg intensities of selected reflections observed in $Tb_{0.97}Y_{0.03}NiAl$ are shown in the upper panel of Fig. 7. Below $T=14$ K only small changes occur due to changing temperatures, but above that point the antiferromagnetic Bragg peaks decrease whereas the ferromagnetic peaks grow remarkably up to about $T=22$ K and then remain almost constant until $T=40$ K. This phenomenon is due to the fact that in certain domains changes from antiferromagnetic to ferromagnetic order occur, when the temperature is increased. In order to estimate the ratio of the volumina ordering ferro- or antiferromagnetically relative to the total volume, an additional assumption is required, namely that magnetic moments in ferromagnetic domains are of the same size as the nonfrustrated (regular) moments in antiferromagnetic domains. At intermediate temperatures the frustrated moments in the antiferromagnetic domains are somewhat reduced in size, which makes it difficult to determine the ratio $V_{\text{afm}}/V_{\text{total}}$ precisely. We arrive at what is shown in the lower panel of Fig. 7. At low temperatures, antiferromagnetism is present in $(76\pm4)\%$ of the volume. The ordered moment is found to amount to $\mu=(7.7\pm0.3)\mu_B$, which seems to be a reasonable value compared to the above mentioned results at $T=2$ K. Below $T=14$ K we observe a plateau for the ratio $V_{\text{afm}}/V_{\text{total}}$. At further increasing temperatures the ferromagnetic domains grow significantly, which is reflected by increasing intensities of the ferromagnetic Bragg peaks. However, the change to ferromagnetism is not complete: At $T=46$ K, about 1 K below the magnetic ordering temperature, antiferromagnetism is still present, and thus both the ferro- and antiferromagnetic states have the same ordering temperature.

The limited resolution of the neutron powder diffractometers $(\Delta q/q\simeq0.01)$ does not allow for a precise determination of the size of the magnetic domains. The line shapes and widths of structural and magnetic Bragg peaks do not look any different. Only in the critical regime, close to the Curie temperature, the typical broadening of the magnetic reflections occurs. From the q resolution a lower limit for the diameter of typical domains of about 300 Å can be estimated.

All compounds with a Y content $x\geqslant0.20$ are Ising ferromagnets. In neutron diffraction experiments no indication for a return to an antiferromagnetic order could be found. The ordering temperature decreases to $T_C=14$ K in $\text{Tb}_{0.20}\text{Y}_{0.80}\text{NiAl}$. The ordered Tb moment also decreases slightly: for $\text{Tb}_{0.20}\text{Y}_{0.80}\text{NiAl}$ at $T=2$ K we found $\mu=(7.3\pm0.4)\mu_B$.

IV. DISCUSSION

The magnetic order in intermetallic compounds with localized $4f$ moments originates from the Ruderman-Kittel-Kasuya-Yosida (RKKY) interaction.[28–32] This was first proposed for the indirect exchange coupling of nuclear spins, but later also applied to rare earth metals,[33] disordered systems,[34,35] and magnetic multilayers.[36] According to this model, magnetic interaction between isolated $4f$ shells is indirectly mediated by conduction electrons. The strength of the RKKY interaction falls off as r^{-3} with increasing relative distance of the moments in question. It is another characteristic of this coupling mechanism that the exchange constant oscillates with respect to the product k_Fr, where k_F is the Fermi wave number (in the original model the Fermi surface is assumed to be spherical). The model was extended in order to hold for more realistic cases,[37] but its main characteristics remained unchanged.

In another indirect magnetic exchange coupling mechanism originally proposed for rare earths and alloys of rare earths and transition metals by Campbell[38] s and d electrons are treated separately. According to this model the coupling between different $4f$ moments is due to a positive spin density in the $5d$ band of the rare earth created by the $4f$ spin and the hybridization of the $5d$ band with the $3d$ band of the transition metal (Ni in our case). The $5d$-$3d$ coupling is antiferromagnetic, because the $5d$ band is almost empty, while the $3d$ band is almost filled. In this situation the binding of the hybridized states is the one with spin densities of different signs in both bands. The net coupling between $4f$ moments is ferromagnetic. In the series $\text{Tb}_{1-x}\text{Y}_x\text{NiAl}$ the paramagnetic Curie-Weiss constants are found to be of the order of $\theta=+30$ K, even for antiferromagnetic TbNiAl. This supports the assumption that Campbell's model, and not pure RKKY, describes the relevant coupling mechanism here.

We have shown that a very unusual transition from antiferromagnetic to ferromagnetic order occurs in the system $\text{Tb}_{1-x}\text{Y}_x\text{NiAl}$. In TbNiAl the sign of the magnetic coupling between nearest neighbors in the ab plane obviously depends on the local environment. Substitution of 1% Tb with Y causes virtually no change in the antiferromagnetic order, while at a Y content as low as 5%, the magnetic order becomes almost completely ferromagnetic. For the same compounds, the expectation value for the distance between neighboring Y sites only changes from 10 Å $(x=0.01)$ to 7 Å $(x=0.05)$, if all 3 dimensions are regarded as equivalent, or from 25 Å $(x=0.01)$ to 11 Å $(x=0.05)$, if only one ab plane is considered. The latter numbers are appropriate, if the magnetic interaction favoring antiferromagnetism is much stronger within one ab plane than between two planes. The crystal structure qualitatively favors this assumption. In TbNiAl Tb-Ni layers and Ni-Al layers alternate along the hexagonal c axis. The closest Tb-Tb distance actually occurs within the ab plane $(d\simeq3.6$ Å$)$. The presence of Ni makes the $5d$-$3d$ hybridization in the same ab plane possible. Finally, the number of nearest neighbors in one ab plane is higher than between two planes, suggesting that the Tb-Tb coupling within one plane is much stronger than between different planes. However, antiferromagnetic ordering of pure TbNiAl requires all three dimensions to be stable. Otherwise the magnetic propagation vector would gradually change from $\boldsymbol{k}_1^{(\text{afm})}=(\frac{1}{2}\frac{1}{2}\frac{1}{2})$ via $\boldsymbol{k}^{(\text{afm})}=(00\frac{1}{2})$ or $\boldsymbol{k}^{(\text{afm})}=(\frac{1}{2}\frac{1}{2}0)$ to $\boldsymbol{k}^{(\text{fm})}=(000)$.

The experimental results reported here are similar to those obtained earlier[20] for the system $\text{TbNi}_{1-x}\text{Cu}_x\text{Al}$. In both cases, the impurities introduced into the system (Y or Cu) sensitively affect the band structure of pure TbNiAl. Y carries three electrons on top of a [Kr] shell ($4d$ and $5s$), but contrary to Tb, it does not have $5d$ or $6s$ electrons. The additional electron Cu carries compared to Ni is believed to fill the Ni $3d$ band, which results in a complete loss of long range magnetic order in $\text{TbNi}_{1-x}\text{Cu}_x\text{Al}$ in the range of $0.60\leqslant x\leqslant0.80$.[20] We conclude that, if the band structure of TbNiAl is perturbed, the magnetic order suddenly changes, when the impurities reach a critical average density, which amounts to about 1% for $\mathrm{TbNi}_{1-x}\mathrm{Cu}_x\mathrm{Al}$ and about 3% for $\mathrm{Tb}_{1-x}\mathrm{Y}_x\mathrm{NiAl}$.

A strong long range magnetic interaction was found in $\mathrm{Tb}_{1-x}\mathrm{Y}_x\mathrm{NiAl}$. A rather slowly declining Curie temperature at increasing Y content supports this assumption: For $\mathrm{Tb}_{0.20}\mathrm{Y}_{0.80}\mathrm{NiAl}$ we found $T_C = 14$ K. Up to $x = 0.70$ pure long range magnetic order was observed by neutron diffraction. There is no indication for the formation of a spin glass state, which would require competing ferro- and antiferromagnetic coupling. This also shows that the RKKY picture in its original form is not appropriate here: Antiferromagnetic order is never reestablished when the content of Cu or Y is further increased. At intermediate and large values of x there is a broad distribution of Tb-Tb distances in the system $\mathrm{Tb}_{1-x}\mathrm{Y}_x\mathrm{NiAl}$. Antiferromagnetic correlations of relevant strength only exist for small values of x, but are increasingly replaced by ferromagnetic correlations with increasing temperatures.

In both series we observed a change of the lattice constants with stoichiometry. This gives rise to the question whether the change of the mean Tb-Tb distance has an important influence on the change of the observed magnetic ordering. This is probably not the case because in the narrow transition regime (3% Y, 1% Cu) this effect is very small and additionally has different signs in both series. At $T = 2$ K and at small x, where the transition from antiferromagnetic to ferromagnetic order occurs, both lattice parameters decrease with x in $\mathrm{Tb}_{1-x}\mathrm{Y}_x\mathrm{NiAl}$, whereas in $\mathrm{TbNi}_{1-x}\mathrm{Cu}_x\mathrm{Al}$ both lattice parameters increase with x. Figure 2 shows that the lattice expansion is anisotropic at room temperature in $\mathrm{Tb}_{1-x}\mathrm{Y}_x\mathrm{NiAl}$: a increases with x, whereas c decreases at the same time. At a fixed stoichiometry, a decreases at decreasing temperature, whereas c increases. This reflects that the interatomic forces which determine positions of the atoms in equilibrium change with temperature and stoichiometry. However, this may not be relevant for the presented investigation.

ACKNOWLEDGMENTS

We would like to thank M. Hoffmann, H. Schneider, and Th. Charvolin for their help during various diffraction experiments. Special thanks are due to W. Rönnfeldt for the preparation of the samples. The authors are greatly indebted to K. Diederichsen for her invaluable assistance in the preparation of the manuscript.

---

*Author to whom correspondence should be addressed. Present address: Institut Laue-Langevin, Boîte Postale 156, 38042 Grenoble, France. Electronic address: ehlers@ill.fr

[1] C. B. Shoemaker and D. P. Shoemaker, Acta Crystallogr. **18**, 900 (1965).

[2] S. Rundqvist and F. Jellinek, Acta Chem. Scand. **13**, 425 (1959).

[3] A. E. Dwight, M. H. Mueller, R. A. Conner, Jr., J. W. Downey, and H. Knott, Trans. Metall. Soc. AIME **242**, 2075 (1968).

[4] E. Hovestreydt, N. Engel, K. Klepp, B. Chabot, and E. Parthé, J. Less-Common Met. **85**, 247 (1982).

[5] A. Szytuła, in *Handbook of Magnetic Materials*, edited by K. H. J. Buschow (North-Holland, Amsterdam, 1991), Vol. 6, p. 85.

[6] V. Sechovský and L. Havela, in *Ferromagnetic Materials*, edited by E. P. Wohlfarth and K. H. J. Buschow (North-Holland, Amsterdam, 1988), Vol. 4, p. 309.

[7] I. Syozi, Prog. Theor. Phys. **6**, 306 (1951).

[8] G. H. Wannier, Phys. Rev. **79**, 357 (1950).

[9] H. Oesterreicher, J. Less-Common Met. **30**, 225 (1973).

[10] N. C. Tuan, thesis, Charles University Prague, 1992.

[11] N. C. Tuan, V. Sechovský, M. Diviš, P. Svoboda, H. Nakotte, F. R. de Boer, and N. H. Kim-Ngan, J. Appl. Phys. **73**, 5677 (1993).

[12] H. Maletta and V. Sechovský, J. Alloys Compd. **207/208**, 234 (1994).

[13] G. Ehlers and H. Maletta, Z. Phys. B **99**, 145 (1996).

[14] P. Javorský, P. Burlet, V. Sechovský, A. V. Andreev, J. Brown, and P. Svoboda, J. Magn. Magn. Mater. **166**, 133 (1997).

[15] G. Ehlers and H. Maletta, Z. Phys. B **101**, 317 (1996).

[16] P. Javorský, P. Burlet, E. Ressouche, V. Sechovský, H. Michor, and G. Lapertot, Physica B **225**, 230 (1996).

[17] P. Javorský, V. Sechovský, R. R. Arons, P. Burlet, E. Ressouche, P. Svoboda, and G. Lapertot, J. Magn. Magn. Mater. **164**, 183 (1996).

[18] A. Dönni, G. Ehlers, H. Maletta, P. Fischer, H. Kitazawa, and M. Zolliker, J. Phys.: Condens. Matter **8**, 11 213 (1996).

[19] K. Prokeš, F. Bourdarot, P. Burlet, P. Javorský, M. Olovec, V. Sechovský, E. Brück, F. R. de Boer, and A. A. Menovsky, Phys. Rev. B (to be published).

[20] G. Ehlers, D. Ahlert, C. Ritter, W. Miekeley, and H. Maletta, Europhys. Lett. **37**, 269 (1997).

[21] Guide to Neutron Research Facilities at the ILL (''The Yellow Book''), ILL, Grenoble, 1997.

[22] Neutron Scattering Instrumentation at the Research Reactor BER II, Berlin Neutron Scattering Centre, 1996.

[23] H. M. Rietveld, J. Appl. Crystallogr. **2**, 65 (1969).

[24] J. Rodriguez-Carvajal, FULLPROF: A program for Rietveld refinement and profile matching analysis of complex powder diffraction patterns (ILL) (unpublished).

[25] V. F. Sears, Neutron News **3**, 26 (1992).

[26] P. J. Brown, *Magnetic Form Factors, International Tables for Crystallography, Vol. C* (Kluwer Academic Publishers, Dordrecht, 1992).

[27] B. Barbara, C. Bécle, R. Lemaire, and D. Paccard, J. Phys. (Paris), Colloq. **32**, C1-299 (1971).

[28] M. A. Ruderman and C. Kittel, Phys. Rev. **96**, 99 (1954).

[29] T. Kasuya, Prog. Theor. Phys. **16**, 45 (1956).

[30] K. Yosida, Phys. Rev. **106**, 893 (1957).

[31] P. G. de Gennes, J. Phys. Radium **23**, 510 (1962).

[32] C. Kittel, Solid State Phys. **22**, 1 (1968).

[33] B. Coqblin, *The Electronic Structure of Rare Earth Metals and Alloys: The Magnetic Heavy Rare Earths* (Academic, London, New York, San Francisco, 1977).

[34] T. Kaneyoshi, J. Phys. F **5**, 1014 (1975).

[35] P. F. de Châtel, J. Magn. Magn. Mater. **23**, 28 (1981).

[36] K. B. Hathaway, in *Ultrathin Magnetic Structures*, edited by B. Heinrich and J. A. C. Bland (Springer, Berlin, Heidelberg, 1994), Vol. 2.

[37] L. M. Roth, H. J. Zeiger, and T. A. Kaplan, Phys. Rev. **149**, 519 (1966).

[38] I. A. Campbell, J. Phys. F **2**, L47 (1972).